Journal of Applied Polymer Science

Flame Retardation of Dibromoneopentyl Glycol on Intumescent Flame-Retardant/Low-Density Polyethylene Composites

Zhi-Ling Ma, Xian-Ling Wang, Hui-Mian Wei, Hong-Zan Song
College of Chemistry and Environmental Science, Hebei University, Baoding 071002, China
Correspondence to: M. Zhi-Ling (E-mail: zhilingma838838@163.com)

ABSTRACT: On the basis of ammonium polyphosphate (APP) microencapsulated with pentaerythritol/dibromoneopentyl glycol (DBNPG) mixed phosphate melamine salt as an intumescent flame retardant (IFR), the influence of DBNPG on the flame retardancy of IFR/low-density polyethylene was investigated. The results prove that DBNPG could influence the combustion heat and the thermal barrier properties of the char layer in combustion. The intumescent degree (ID), compactness, and closure were the determinants of the thermal barrier properties of the char layer. A greater ID below 500°C and then a more compact and closed char layer above 500°C contributed to the better thermal barrier properties. An appropriate DBNPG reduced the combustion heat and promoted the formation of a compact and closed char layer by increasing of the melting viscosity of the composites. However, excessive DBNPG destroyed the closure of the char layer and increased the combustion heat because of a decrease in the melting viscosity of the composites. © 2014 Wiley Periodicals, Inc. J. Appl. Polym. Sci. **2015**, *132*, 41244.

KEYWORDS: composites; properties and characterization; thermogravimetric analysis (TGA); viscosity and viscoelasticity

Received 6 January 2014; accepted 29 June 2014
DOI: 10.1002/app.41244

INTRODUCTION

Intumescent flame retardants (IFRs), with many merits, such as a low generation of toxic smoke during burning, are widely used. The intumescent flame retardant system (IFRS) consists of three essential factors: an acid source, a carbonization agent, and a blowing agent. A typical IFRS consists of ammonium polyphosphate (APP), pentaerythritol (PER), and melamine (M). However, the hydrophilicity of the three ingredients results in the active ingredients are moisture-sensitive and capable of migration to the surface of the composites, and this limits their flame retardancy. Therefore, many researchers have devoted to the investigation of highly polymerized microcapsule APP[1,2] to obtain better hydrophobic properties. Meanwhile, to overcome the shortcomings of PER and M, some studies have been carried out. The spirocyclic pentaerythritol di(phosphate melamine salt) with the commercial name CN-329 was synthesized from phosphorus oxychloride, PER, and M;[3] this concentrated the three essential factors of IFRS in one molecule. However, the environmentally unfriendly HCl was produced concomitantly. In our previous study, an IFR was synthesized by a water-insoluble pentaerythritol phosphate melamine salt made from phosphorus pentoxide (P_2O_5), PER, and M; this microencapsulated APP[4–6] and minimized leaching problems and has been effectively used in flame-retarded polypropylene, although in flame-retarded low-density polyethylene (LDPE) a high loading of IFR resulted in a poor compatibility that deteriorated the performance of the IFR/LDPE. Therefore, to enhance the flame retardancy and decrease the high loading, the need to explore the production of more sufficient flame retardant is urgent.

The flame-retardant mechanism as a foundation for enhancing the flame retardancy has attracted more and more attention. It has been confirmed that the melting viscosity of composites,[7] the synergetic effect of the flame-proofing elements,[8,9] and the thermal intumescent factor of a material[10] are closely related to the flame retardancy of composites. Dibromoneopentyl glycol (DBNPG), as a brominated flame retardant, was developed in the 1970s. The products, such as flame-retarded polyesters[11,12] and phosphates,[13,14] synthesized from DBNPG have been studied extensively. With a low bromine content, characteristic quaternary carbon atom, and dihydroxyl structure, DBNPG can act as the carbon source in IFRSs. In this project, DBNPG partly replacing PER was introduced into an IFR that was applied to flame-retarded LDPE. The flame-retardant mechanism of the IFR/LDPE was explored through the effect of DBNPG on the flame retardancy, rheological behaviors, char residue, and thermal degradation of the IFR/LDPE. The research results are expected to make a contribution to decreasing the loading of IFRs and developing more efficient flame-retarded materials.

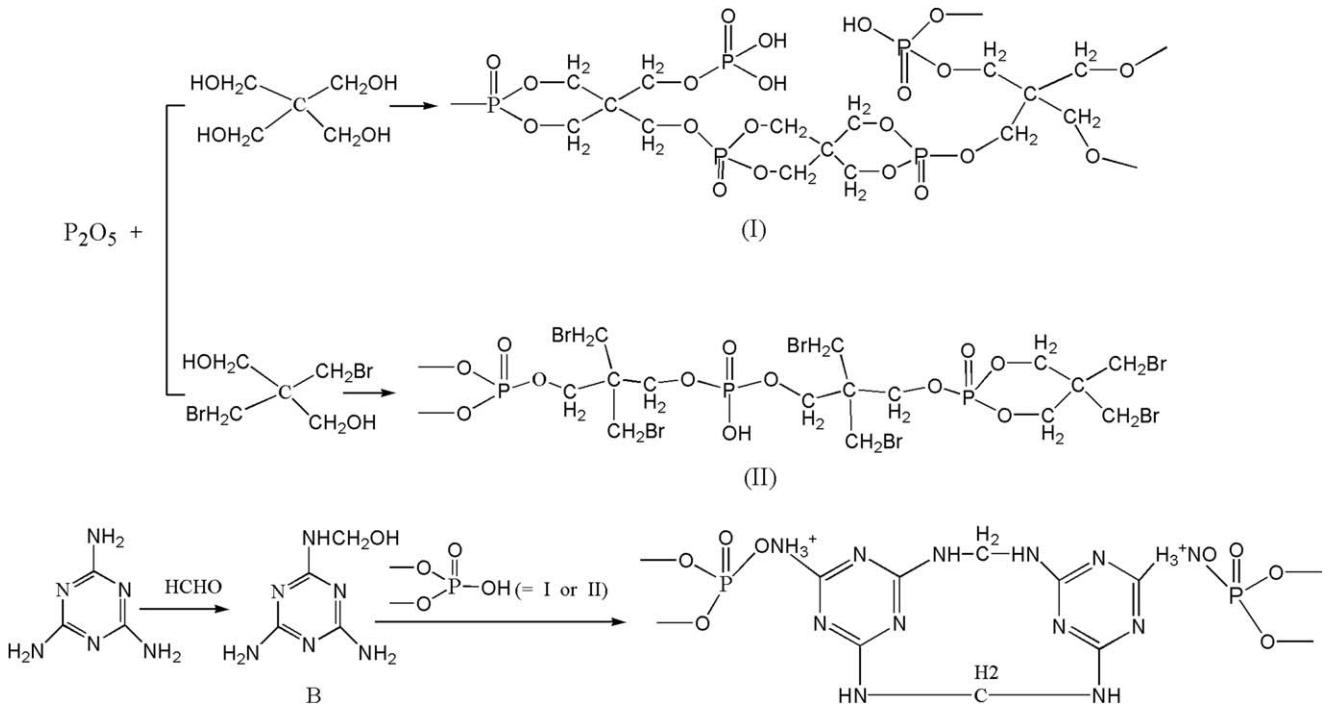

Scheme 1. Relevant reactions of IFRs.

EXPERIMENTAL

Materials

LDPE (LD100-AC, density = 0.9225 g/cm^3, melt flow index = 0.2 g/min^3) was supplied by Petro China Co., Ltd., Daqing Branch (Daqing, China). DBNPG (970I) was provided by Linan Chemical Co., Ltd., of Zhejiang Province (Hangzhou, China). P_2O_5 (≥99.0%) was provided by Gaolong Phosphorus Chemical Industry Co., Ltd. (Xiangfan, China). PER (≥95.0%) was obtained from Ruiyang Chemical Co., Ltd. (Liyang, China). APP (FR-II) was supplied by Shanghai Xusen Non-Halogen Smock Suppressing Fire Retardants Co., Ltd. (Shanghai, China). M (≥99.8%) was obtained from Jinan Taixing Chemical Co., Ltd. (Jinan, China). Formaldehyde (≥37.0%) was an analytical reagent purchased from Tianjin Kemiou Chemical Reagent Co., Ltd. (Tianjin, China).

Synthesis of the IFRs

The IFRs were prepared according to the following procedure and with the relevant reactions shown in Scheme 1. The calculated proportions for the main components of the IFRs, such as, P_2O_5, pentaerythritol phosphate (PER-P), and dibromoneopentyl glycol phosphate (DBNPG-P), are listed in Table I.

Primarily, 131.8 g of P_2O_5 and the mixture of DBNPG/PER weighed as shown in Table I were added alternately to a four-necked glass flask equipped with a stirrer, thermometer, and reflux condenser at 110°C, and then, the temperature was gradually increased to 140°C. The reaction was continued for about 4 h. When the acid value could not be decreased, the reaction was stopped, and the products A0–A3 were ready to be used.

Second, 70.2 mL of formaldehyde and 117.0 g of M were reacted at 85°C for 30 min, and the product B was ready to be used.

Finally, IFR0 was prepared according to the following procedure: 358.8 g of APP was dispersed in 200 mL of water, products A0 and B were added alternately, then the temperature was gradually increased to 70°C, and the reaction was continued for 1 h. The products were cooled, filtered, dried, and crushed successively, and IFR0 was ready to be used.

IFR1, IFR2, and IFR3 were prepared by the same procedure as IFR0 with the addition of product A1, A2, or A3, respectively, instead of A0.

Preparation of the IFR/LDPE Composites

Before blending, the IFR was shattered by a gas flow ultramill (RT-25, Beijing Yanshan Zhengde Machinery Equipment Co., Ltd., China), and the granularities of the powders were about 12–44 μm. The IFR/LDPE composites were prepared, respectively, with an IFR/LDPE ratio of 35/65 by melt-blending on a two-roll mill (Yicheng Shoe Machine Co., Ltd., China) at around 140°C. After the LDPE melted, the IFR powders were added. Then, the composites were mixed for 10 min and moved for compression molding at 120°C for 3 min. Finally, the composites were cooled to room temperature by cool pressing. After being annealed at 70°C for 8 h, the specimens were operated on

Table I. Characteristic Compositions of IFRs

IFR	PER (g)	DBNPG (g)	W_{P2O5} (%)	W_{PER-P} (%)	$W_{DBNPG-P}$ (%)
IFR0	100.0	0	52.1	32.8	0
IFR1	90.0	38.5	50.1	28.3	7.0
IFR2	80.0	77.0	48.3	24.3	13.5
IFR3	70.0	115.5	46.6	20.5	19.6

W = mass fraction of main components of the IFRs.

Table II. IFR/LDPE Property Test Results

			Horizontal combustion tests			ID (cm^3/g)		
Composite	TS (MPa)	BE (%)	BP		ET (s)	350°C	450°C	500°C
A. LDPE	10.2	369.5	Burn, dripping	—	—	—	—	—
B. IFR0/LDPE	6.2	61.4	Intumescing	FH-1	30	7.9	11.6	2.1
C. IFR1/LDPE	6.3	84.2	Intumescing	FH-1	27	4.6	5.0	1.7
D. IFR2/LDPE	7.8	82.1	Intumescing	FH-1	19	5.8	7.4	1.4
E. IFR3/LDPE	6.5	76.8	Bending	FH-1	21	5.5	6.3	1.9

an almighty sample-preparing machine (ZHY-W, Chengde Experimental Factory, China).

Flame Retardancy and Tensile Properties

The horizontal combustion tests were carried out on a CZF-3 instrument (Nanjing Qionglei Equipment Co., Ltd., China) according to GB/T 2408-2008. The burning phenomena (BP) and extinguish time (ET) are recorded in Table II.

In a 350, 450, and 500°C muffle furnace for 5 min, the specimen (ca. 1.000 g) volumes were measured before and after heating in 25-mL crucibles. We measured the irregular carbon layer by cutting the sample into squares according to the cabinet method tests of fire-retardant coatings (GB/T12441-2005). The intumescent degree (ID) of the specimens were calculated with the following formula:

$$\mathrm{ID}\left(\frac{\mathrm{cm}^3}{\mathrm{g}}\right)=\frac{\text{Volume after heating}-\text{Volume before heating}}{\text{Sample mass}}$$

The tensile properties were measured with an LJ-5000N mechanical tensile testing machine (Chengde Testing Machineries Factory, China) with a crosshead speed of 50 mm/min according to GB/T 1040-2006. The data of the tensile strength (TS) and breaking elongation (BE) are listed in Table II.

In the aforementioned several measurements, at least five samples for each test were usually analyzed to obtain reproducible results and determine the average values.

Rheological Behaviors

The rheological behaviors were measured with an AR2000ex stress-controlled rheometer with a 25-mm parallel-plate geometry (TA Instruments). Temperature sweep measurements were carried out with a fixed frequency of 6.28 rad/s, and the samples were scanned from 145 to 250°C with a heating rate of 2°C/min. All measurements were conducted under a nitrogen atmosphere. To ensure data accuracy and repeatability, three measurements were carried out for each sample.

Thermal Analysis

Thermal analysis was performed with an HCT-3 standard thermogravimetry (TG)-dynamic thermal analysis (DTA) instrument (Beijing Henven Scientific Instrument Factory, China), The samples were examined under air flowing at 30 mL/min with a heating rate of 10°C/min and a temperature that ranged from 50 to 800°C. The masses of samples A–E were 8.5, 7.5, 7.4, 7.5, and 6.8 mg, respectively. With high-purity zinc as the standard, the heat release in the relevant temperature ranges of the DTA curves were calculated by the Beijing Henven thermal analysis software and are shown in Table III. Differential scanning calorimetry (DSC) for the IFR powder with a PerkinElmer Precisely DSC-7 analyzer at a heating rate of 50°C/min under a static nitrogen atmosphere was measured from 50 to 180°C.

Scanning Electron Microscopy (SEM)

The morphology of the impact rupture surface for composites was observed with a KYKY-2800B scanning electron microscope (KYKY Technology Development, Ltd., China).The impact rupture surface was obtained from brittle fracturing with refrigerated liquid nitrogen. The surface of the composites were previously coated with a conductive layer of gold.

The char residues formed after horizontal combustion testing were observed by a Hitachi TM 3000 emission scanning electron microscope (Japan) with an acceleration voltage of 15.0 kV.

RESULTS AND DISCUSSION

Flame Retardancy and Tensile Properties

The horizontal combustion tests showed that the virgin LDPE was flammable, and it dripped during burning. After mixed the IFR, the test results of all of the composites reached the FH-1

Table III. Results of the IFR/LDPE TG and DTA

		Char yield (%)				DTA	
Composite	$T_{5\%}$ (°C)	300°C	450°C	500°C	600°C	H_i (mJ/mg)	
A. LDPE	359	100	41.6	3.1	3.0	250–430°C	1022.3
B. IFR0/LDPE	335	98.1	59.5	15.2	14.4	230–480°C	666.7
C. IFR1/LDPE	349	98.7	80.0	16.8	16.2	230–480°C	102.6
D. IFR2/LDPE	376	100	77.9	27.3	27.1	230–480°C	90.5
E. IFR3/LDPE	370	100	81.5	25.6	25.1	230–480°C	125.0

H_i = heat release in the relevant temperature ranges (i = A,B,C,D,E).

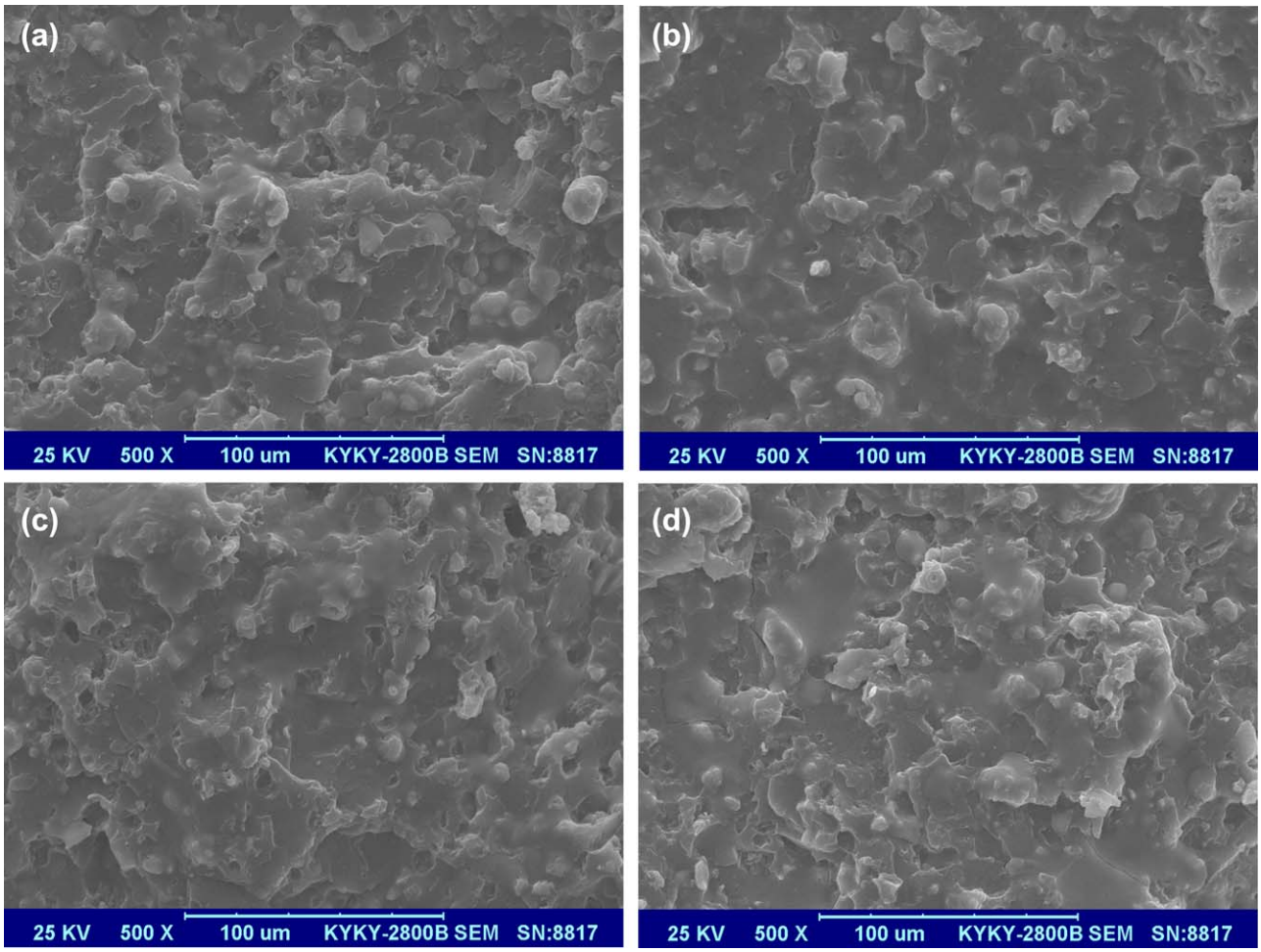

Figure 1. SEM images of the impact rupture surfaces of the IFR/LDPE composites: (a) sample B (IFR0/LDPE = 35/65), (b) sample C (IFR1/LDPE = 35/65), (c) sample D (IFR2/LDPE = 35/65), and (d) sample E (IFR3/LDPE = 35/65). [Color figure can be viewed in the online issue, which is available at wileyonlinelibrary.com.]

categories. Composite B was intumescent and extinguished without dripping. However, the results of the tensile properties showed that the TS and BE of composite B decreased by 39.2 and 83.4%, respectively, compared with those of the virgin LDPE. With the introduction of DBNPG, the ET values of the composites were further shortened. More specifically, we noticed that composite D achieved an ET of 19 s, and even the TS and BE were strengthened by 25.8% and 33.7%, respectively, compared to those of composite B.

The strengthened tensile properties were due to the enhanced interfacial adhesion of IFR/LDPE caused by the introduction of DBNPG. As shown in Figure 1, the impact rupture surface of the composites was observed by SEM to investigate the interfacial adhesion of the IFR and LDPE. The impact rupture surface of composite B was rough, with many naked particles accumulating on it. The impact rupture surface was more inclined to the interface of IFR0 and LDPE; this suggested poor adhesion between them. When DBNPG was added, the IFR was dispersed homogeneously, and the interface of IFR and the LDPE matrix became less well defined from composites C to E. We concluded that DBNPG had a compatibilization effect on the enhanced interfacial adhesion of IFR and LDPE.

Figure 2 reveals the results of the horizontal combustion test of the IFR/LDPE composites. As the photos show, the composites formed an intumescent char residue covering the surface to efficiently protect the substrate from flames. Composite B was bent slightly, composites C and D were not bent, and it was obvious that the char residue of composite D showed perfect integrity. However, composite E was bent and tended to form droplets. The experiment phenomena demonstrated that an appropriate amount of DBNPG introduced into the IFR played an important role in dripping resistance. However, an excess of DBNPG had a negative effect on the dripping resistance, which worsened the integrity of the char residue and the flame retardancy of the composites. Further works are still in progress to examine this.

Morphology of the Char Residue

Figure 3 shows the morphology of the char residue after the horizontal combustion test. The expanded shape residue of composite B showed that the size of the intumescent bubbles was nonuniform; in some places, the bubbles were small and thick-walled, but they were large and even open with thin walls in other places. Because of the compatibilization effect of DBNPG, the size distribution of thee intumescent bubbles

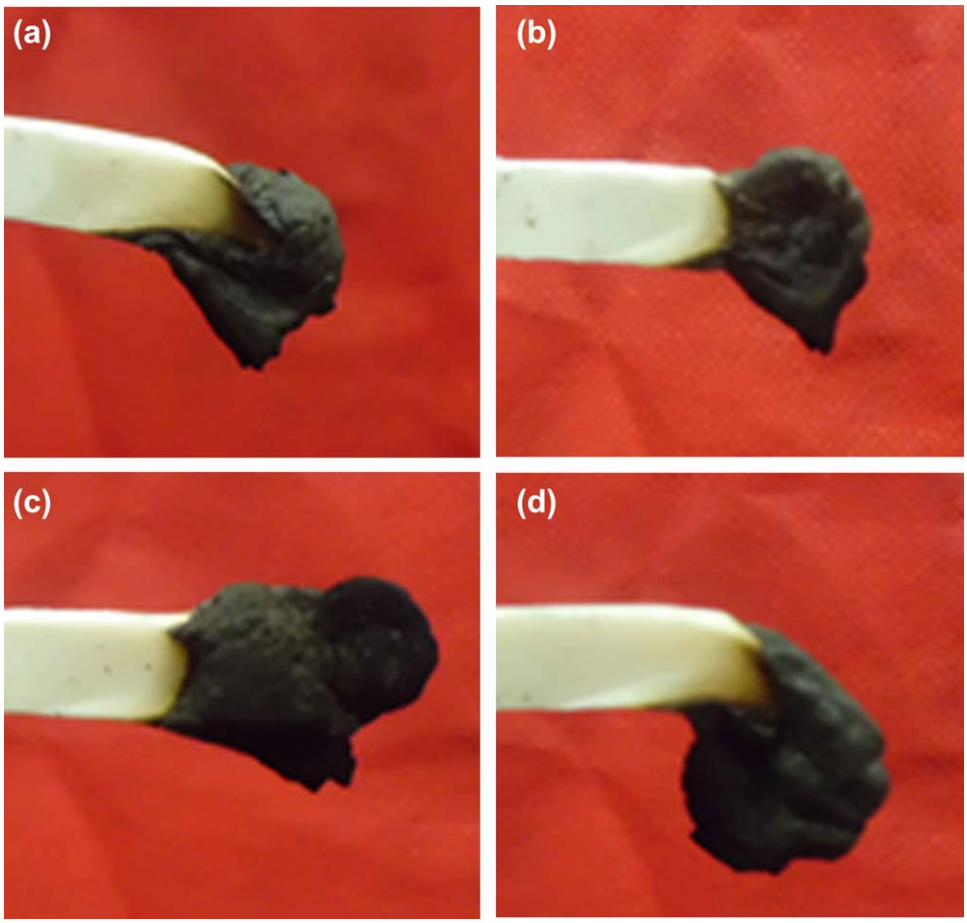

Figure 2. Burning behavior of IFR/LDPE: (a) sample B, (b) sample C, (c) sample D, and (d) sample E. [Color figure can be viewed in the online issue, which is available at wileyonlinelibrary.com.]

became narrow and uniform, The char residues of composites C and D showed thick-walled bubbles. In particular, composite D showed excellent compact and closed char layers with lots of tiny carbon particles accumulating on the bubble's surface. However, the char residue of composite E exhibited showed open and thin-walled bubbles.

The results of SEM prove that the content of DBNPG influenced the IFR dispersability in LDPE and the char residue morphology. When the proportion of PER/DBNPG was 80.0/77.0, the composite showed good compatibility and formed a compact closed-bubble char layer during heating; this was very important for the flame protection of the underlying materials. Because the compact closed-bubble formation meant that the combustible gases released from the degradation were trapped in the melt-degraded char residue. This not only provided an excellent thermal barrier but also significantly reduced heat transfer and air incursion during combustion. To explore the sufficient flame-retardant mechanism, more experiments need to be done.

Rheological Behaviors of IFR/LDPE

From the DSC curves in Figure 4, we can see that from IFR0 to IFR3, the starting softening temperature of the IFRs tended to decrease gradually. This may have been because the soft-segment structure of the IFR was increased because of the increased proportion of DBNPG-P, as shown in Table I.

When the dihydroxy DBNPG was substituted for the tetrahydroxy PER of the IFR, on the one hand, this enhanced the interaction between LDPE and IFR; on the other hand, it decreased the starting softening temperature of the IFR. These two factors had the opposite effects on the melting viscosity of the composites. Figure 5 shows the complex melting viscosity of the composites between 145 and 250°C.

In the temperature range of 145–180°C, for composites B, C, and D, the changing trend of the melting viscosity with temperature basically was the same as that of pure LDPE; this indicated that the melting viscosity changing trend of the composites mainly relied on that of LDPE. As a result of the enhancement of the interaction between LDPE and IFR by means of the introduction of DBNPG, the melting viscosities of composites C and D increased successively compared to that of composite B. Above 180°C, the IFRs almost melted completely, and the melting viscosity of composite B decreased rapidly with increasing temperature because of the poor compatibility of IFR0 and LDPE. Because DBNPG improved the interfacial adhesion of LDPE and IFR, the melting viscosities for composites C and D increased successively. Because of the low starting

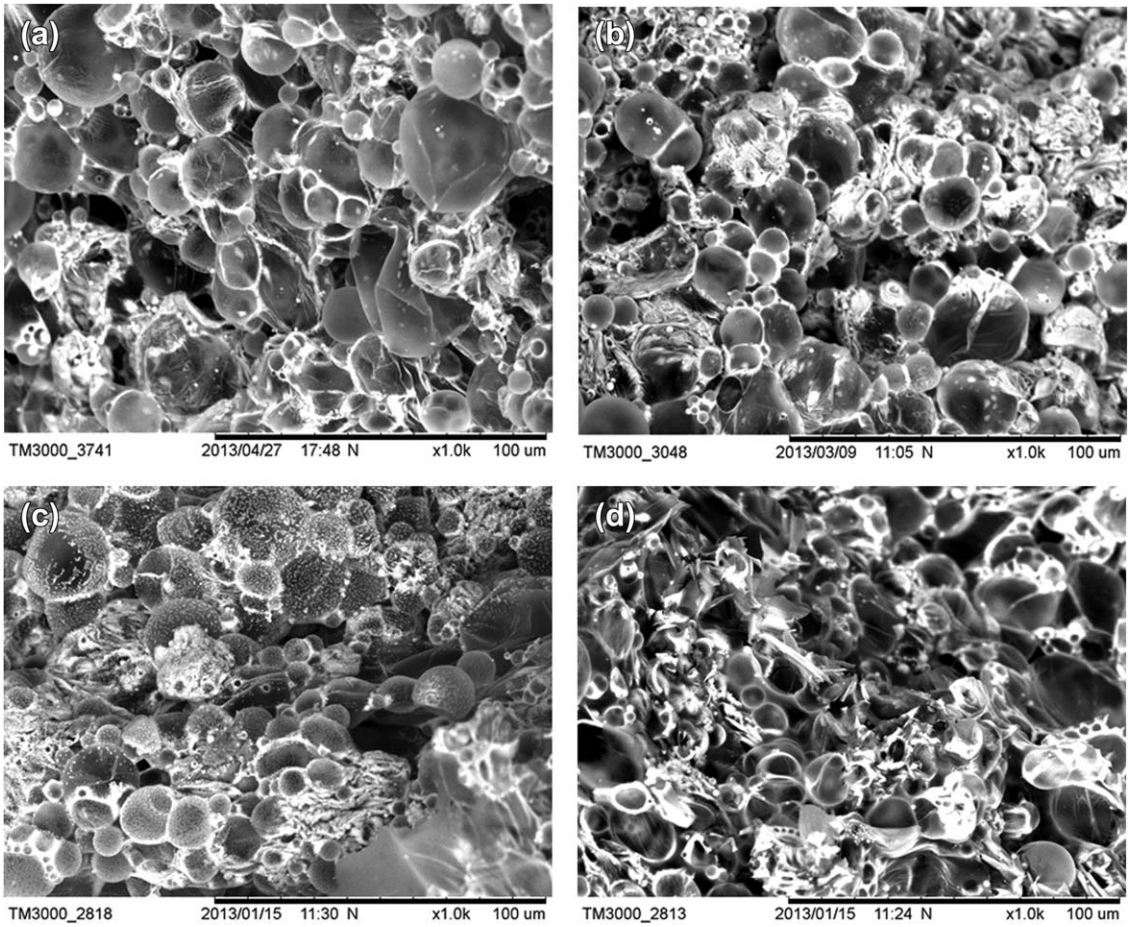

Figure 3. SEM micrographs of the residual char after the horizontal combustion test: (a) sample B (IFR0/LDPE = 35/65), (b) sample C (IFR1/LDPE = 35/65), (c) sample D (IFR2/LDPE = 35/65), and (d) sample E (IFR3/LDPE = 35/65).

softening temperature for IFR2 and IFR3, the decreasing speed of the melting viscosity of composites D and E with temperature gradually accelerated from the lower temperature, and the melting viscosity curve of composite E was below that of composite D.

It was clear that appropriate DBNPG added to IFR increased the melting viscosity of IFR/LDPE. A high melting viscosity was reported to promote the formation of a compact and closed cellular foam char layer and to restrict the transmission both heat and flammable gases.[7,10] Furthermore, a high melting viscosity

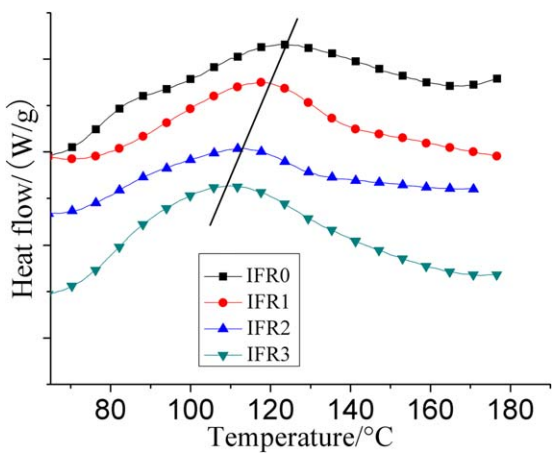

Figure 4. DSC curves of the pure IFR powder. [Color figure can be viewed in the online issue, which is available at wileyonlinelibrary.com.]

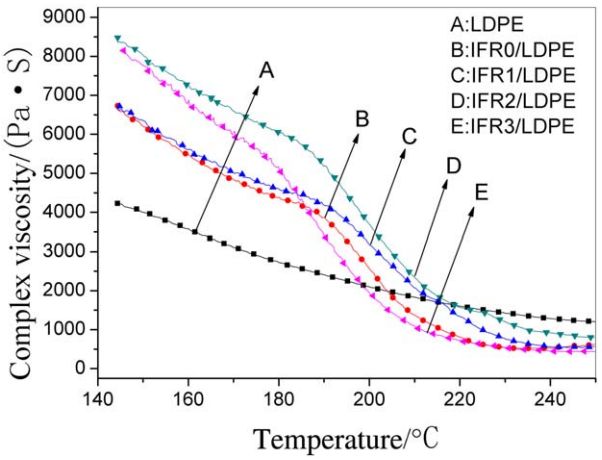

Figure 5. Rheological behavior of IFR/LDPE. [Color figure can be viewed in the online issue, which is available at wileyonlinelibrary.com.]

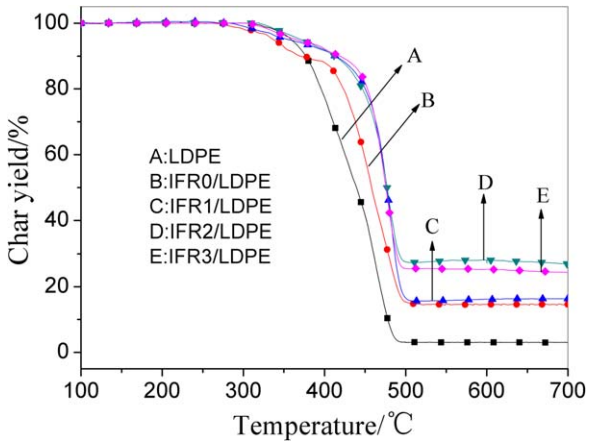

Figure 6. TG curves of IFR/LDPE. [Color figure can be viewed in the online issue, which is available at wileyonlinelibrary.com.]

could prevent the composite bending in combustion; this is beneficial for the formation of an integral char layer, which effectively protects the underlying materials. These were proven by the foregoing flame-retardancy tests.

Thermal Analysis

Thermal analysis is an effective method for investigating the thermal degradation behavior of fire-retardant materials. Generally speaking, a high char yield and low exothermic heat are advantageous to the flame retardancy. As far as intumescent flame-retarded materials are concerned, the thermal barrier properties of the intumescent char layer has a decisive influence on the temperature at the point of the sample and the shape of the DTA curve.[15,16]

The TG and DTA results are shown in Figures 6 and 7 and Table III. As shown in Figure 6, the polyethylene chain of LDPE decomposed from 250 to 480°C. The thermal degradation of IFR/LDPE occurred in two successive stages. The first stage, from 230 to 500°C, with the greatest mass loss ratio, was generally accepted as the intumescent process. In this stage, the thermal degradation of the polyethylene chain was delayed because of the thermal barrier effect of the char layer. As a result, the char yields of the composites were increased, and the exothermic peaks in the DTA curves tended to be more gentle than that of virgin LDPE. The second step from 500°C was assigned to the degradation of the intumescent structure, probably via oxidative reactions.

As shown in Table III, the temperatures of 5 wt % mass loss ($T_{5\%}$'s) for composites C, D, and E increased by 14, 41, and 35°C, respectively, compared with that for composite B. Between 300 and 450°C,the weight losses of composites B, C, D, and E were 38.6, 18.7, 22.1, and 18.5%, respectively. We inferred that the introduction of DBNPG promoted the thermal stabilization of IFR/LDPE and delayed the intumescent process.

It is generally known that a low mass loss stands for good thermal barrier properties of the char layer. Between 450 and 500°C, the mass losses of composites B, C, D, and E were 44.5, 63.2, 50.6, and 55.9%, respectively. Therefore, the thermal barrier properties of the char layer were ranked as B > D > E > C. It can be seen from Table II that the ID ranking of the composites at 350 and 450°C was B > D > E > C. We confirmed that below 500°C, the IDs of composites were the major determinant of the char layer's thermal barrier properties: the greater the ID was, the better thermal barrier properties were.

As the temperature rose between 500 and 600°C, the mass losses of composites B, C, D, and E were 0.8, 0.6, 0.2, and 0.5%, respectively; this implied that the development of the intumescent process was almost finished, and the thermostable char layer was formed with excellent thermal barrier properties in this temperature range. The thermal barrier properties were ranked as D > E > C > B. The data in Table III show that DBNPG increased the char yields of the composites at 500 and 600°C. Meanwhile, the ID of composites at 500°C in Table II was ranked B > E > C > D. It was not difficult to conclude that the higher the char yield and the lower the ID were, the more compact the char layer was. When the results of SEM were combined, the char layer of composite D showed the optimal compactness and closure properties. Consequently, above 500°C, the char layer's compactness and closure were the determinants of the thermal barrier properties; the more closed and compact the char layer was, the more effective the thermal barrier properties were.

The combustion heat in degradation was considered to be another important parameter for the flame-retarded materials because the lower combustion heat feedback to the material surface decreased the pyrolysis of the material and the flame-spread rate. The DTA traces and relevant data are shown in Figure 7 and Table III, respectively. In the range of 230–500°C, the thermal intumescent stage, with increasing content of DBNPG, the exothermic peaks in the DTA traces of composites C and D successively flattened. In particular, composite D showed the minimum exothermic heat. However, excessive DBNPG increased the heat release of composite E. Above 500°C, the thermal intumescent process was almost complete, and the exothermic peaks in that range suggested the char layer's thermal barrier properties. The second exothermic peak of composite C was obviously broadened; this implied that the

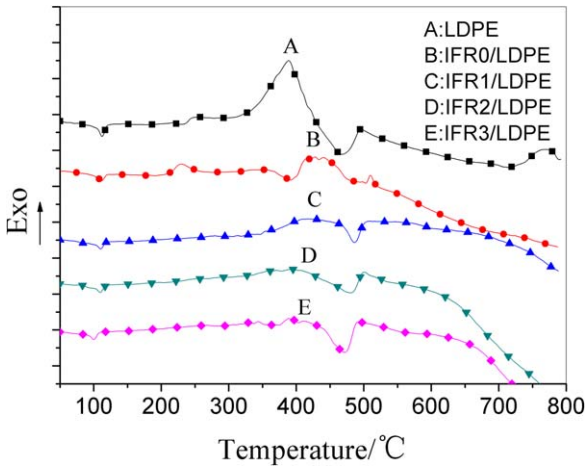

Figure 7. DTA traces of IFR/LDPE. [Color figure can be viewed in the online issue, which is available at wileyonlinelibrary.com.]

char layer's thermal barrier properties were effectively enhanced. It was noteworthy that although the exothermic peak of composite D was narrow, the peak height was reduced; this showed the excellent thermal barrier properties. However, the exothermic peak of composite E was higher than that of composite D; this suggested that the thermal barrier properties of the char layer were weakened.

Flame-Retardant Mechanism

The flame retardancy of the IFR/LDPE was closely related to the combustion heat and the thermal barrier properties of the char layer in combustion.

The acid source, as one of the three essential factors of an IFRS, played the catalytic role in the intumescent process. Because of the high P_2O_5 proportion of IFR0 (Table I), the intumescent process of composite B was accelerated; this contributed to the greater ID of the char layer below 450°C. Therefore, the further decomposition between 450 and 500°C showed restricted availability; this resulted from the char layer's thermal barrier effect. However, the pentaerythritol phosphate melamine salt of IFR0 was badly compacted with LDPE; this resulted in IFR0 being dispersed in a nonuniform manner in the LDPE. The melting viscosity of the composite was low in the place where less IFR0 dispersed; this led to the formation of an opened and thin-walled intumescent char layer displaying poor thermal barrier properties, and the flame retardancy of the composite materials was deteriorated.

When an appropriate amount of DBNPG was introduced, on the one hand, because of the lower proportion of P_2O_5, the intumescent processes below 450°C of composites C, D, and E were restricted and confined mainly to 450–500°C. On the other hand, the interaction of IFR and LDPE was enhanced; this promoted the IFR being dispersed homogeneously in LDPE, and the melting viscosity of IFR/LDPE was increased. These properties were advantageous to the formation of a closed and compact char layer with excellent thermal barrier properties. The degradation gases were trapped in the high-viscosity melt, and the flammable products were effectively inhibited. Also, the HBr produced by DBNPG in burning efficiently catched the highly reactive HO· and inhibited the combustion chain reaction in the gas phase. As a result, the intumescent process exothermic heat of composites C and D was greatly reduced in succession. However, the excessive linear DBNPG in IFR3 lowered the melting viscosity of composite E; this was harmful to the thermal barrier properties of the intumescent char layer with opened and thin-walled bubbles. Meanwhile, the low melting viscosity broke the integrity of the char and led to the underlying materials being exposed to flame, and the flame retardancy of the materials was deteriorated.

CONCLUSIONS

The effects of DBNPG on the flame retardancy of IFR/LDPE were reflected in the combustion heat and the thermal barrier properties of the char layer in combustion. The ID, compactness, and closure were the main determinants in the thermal barrier properties of the char layer. Below 500°C, the greater ID contributed to better thermal barrier properties. Above 500°C, the closed and compact char layer made for excellent thermal barrier properties.

A high proportion of P_2O_5 was beneficial to the greater ID of the char layer. An appropriate amount of DBNPG increased the melting viscosity and the char yield of IFR/LDPE; this contributed to the formation of a closed and compact char layer and reduced the combustion heat. All of these enhanced the fire retardancy of the IFR/LDPE. However, excess DBNPG had the opposite effects. In summary, when the DBNPG/PER ratio was around 77.0/80.0 and the IFR/LDPE ratio was 35/65, the composite exhibited optimal fire resistance with excellent mechanical properties.

REFERENCES

1. Bourbigot, S.; Bras, L. B.; Duquesne, S.; Rochery, M. *Macromol. Mater. Eng.* **2004**, *289*, 499.
2. Wang, Z. Z.; Wu, K.; Hu, Y. *Polym. Eng. Sci.* **2008**, *48*, 2426.
3. Zhu, G. J.; Liu, G. T.; Wang, X.; Yang; X. J.; Lu, L. D. *J. Nanjing Univ. Sci. Technol.* **2002**, *26*, 76.
4. Ma, Z. L. ZL 10,128019.7, China (**2008**).
5. Zhang, P.; Song, L.; Lu, H. D.; Hua, Y.; Xing, W. Y.; Ni, J. X.; Wang, J. *Polym. Degrad. Stab.* **2009**, *94*, 201.
6. Liu, Y.; Wang, D. Y.; Wang, J. S.; Song, Y. P.; Wang, Y. Z. *Polym. Adv. Technol.* **2008**, *19*, 1566.
7. Jimenez, M.; Duquesne, S.; Bourbigot, S. *Surf. Coat. Technol.* **2006**, *201*, 985.
8. Ren, Q.; Wan, C. Y.; Zhang, Y.; Li, J. *Polym. Adv. Technol.* **2011**, *22*, 1414.
9. Skinner, G. A.; Parker, L. E.; Marshall, J. *Fire Mater.* **1976**, *1*, 154.
10. Wang, G. J.; Yang, J. Y. *Surf. Coat. Technol.* **2012**, *206*, 2149.
11. Ou, Q. R.; Li, Y. Y. *Plast. Additives* **2004**, *6*, 31.
12. Skinner, G. A.; Haines, P. J.; Lever, T. J. *J. Appl. Polym. Sci.* **1984**, *29*, 763.
13. Ma, Z. L.; Cui, H. X.; Ji, G. N. *China Plast.* **2007**, *21*, 72.
14. Halpern, Y. U.S. Pat. 279,659 (**1982**).
15. Ma, Z. L.; Fan, C. R.; Lu, G. Y.; Liu, X. Y.; Zhang, H. *J. Appl. Polym. Sci.* **2012**, *125*, 3567.
16. Witkowski, A.; Stec, A. A.; Hull, T. R. *Polym. Degrad. Stab.* **2012**, *97*, 2231.